*Macromol. Symp.* ***184**, 1–18 (2002)*

# New Insights into the Development of Ordered Structure in Poly(ethylene terephthalate), II Results from Transmission Infrared Spectroscopy of Thin Films

*Kenneth C. Cole*, Abdellah Ajji, and Éric Pellerin*

Industrial Materials Institute, National Research Council Canada
75 De Mortagne Blvd., Boucherville, Quebec, Canada J4B 6Y4

**Summary:** To complement our earlier work involving external reflection infrared spectroscopy of PET, a set of thin PET films with different crystalline structures (amorphous, strain-induced crystallinity, thermally induced crystallinity) was prepared and analyzed in detail in the transmission mode. In analogy with the reflection work, factor analysis was used to generate three basis spectra corresponding to three distinct structures: G = an arrangement involving *gauche* glycol conformers and disordered terephthalate groups; TX = an arrangement involving *trans* glycol conformers and disordered terephthalate groups (probably a mixture of *cis* and *trans* conformers); and TC = the all-*trans* arrangement found in the true crystalline phase. The TX structure is believed to play an important role in the widely reported "intermediate" phase of PET, which is particularly significant in cold-drawn samples. The transmission spectra confirm the validity of the reflection spectra and also provide more detailed information. In addition, analysis of two biaxially oriented industrial films has provided further information on the geometry of certain vibrational modes. Overall, the results lead to a better understanding of the complex crystalline structure of PET and its relationship to the infrared spectrum.

## Introduction

The molecular conformation plays an important role in determining the structure and processing behaviour of the widely used semicrystalline polymer poly(ethylene terephthalate), or PET. Previous work aimed at elucidating this role was reviewed in Part I.[1] It is widely accepted that the main conformational change involves the ethylene glycol segment of the molecular chain, which in amorphous PET exists predominantly in the *gauche* (G) form with respect to rotation about the C–C bond, but in crystalline PET exists entirely in the *trans* (T) form. However, different conformational states can also exist for the C–O bond of the glycol group, which can likewise exist in *gauche* (g) and *trans* (t) forms, as well as for the terephthalic acid segment of the molecular chain. In the latter case, the two carbonyl groups adjacent to

CCC 1022-1360/00/$ 17.50+.50/0

the benzene ring either can lie in the same plane as the ring, in which case they may be either *cis* ($C_B$) or *trans* ($T_B$) with respect to each other, or they can lie out of the plane. For the crystalline phase, X-ray measurements have shown that all three groups adopt the *trans* conformation (T, t, $T_B$); this results in a molecule that is very close to planar, except for the glycol hydrogen atoms, leading to efficient packing in the crystal.[2] In the amorphous phase the situation is less well defined but studies have suggested that the conformational distribution is approximately as follows: G : T = 90:10, g : t = 26:74, and $C_B : T_B$ = 50:50.[3]

Many studies have indicated that PET cannot be described in terms of a simple two-phase amorphous-crystalline system, and that values obtained for the crystalline content depend very much on the method used to measure it. To explain this, the existence of an "intermediate" phase is often proposed, but the exact nature of this phase has not been clearly established. In Part I we described a study of a set of PET samples by external reflection infrared (IR) spectroscopy. [1] This approach has the advantage of accurately representing the most intense peaks in the IR spectrum, which are often saturated or distorted in transmission and internal reflection studies. The samples included highly amorphous (quenched) material, samples thermally crystallized at different temperatures, and samples with strain-induced crystallinity achieved by drawing at 80°C. Factor analysis of the spectra led to three principal factors that were combined to give three distinct "basis spectra" designated G, TX, and TC. The G spectrum corresponds to units of the molecular chain containing *gauche* glycol conformers, found in large proportion in the amorphous phase. The TC spectrum corresponds to the fully *trans* conformation found in the true crystalline phase. The TX spectrum corresponds to an intermediate state of order in which the glycol conformers are *trans*, as in the crystalline phase, but the terephthalate segments are disordered, as in the amorphous phase. The TX structure is particularly important in the drawn samples; it corresponds to both isolated *trans* units found in the amorphous phase and to extended *trans* sequences found in the "intermediate" phase. It was not clear from the TX spectrum whether the terephthalate segments possess out-of-plane arrangements or a mixture of *cis* and *trans* planar arrangements.

Although external reflection can provide interesting data concerning the strongest peaks in the spectrum, the somewhat higher noise level limits the information available from the weaker peaks. In order to overcome this problem and obtain complementary information, a new set of samples based on thin films was prepared and analyzed in the transmission mode.

## Experimental

The PET used was the same as in our previous work, namely DuPont Selar PT 7086. Thin films with very low crystallinity and negligible orientation were obtained by extrusion blowing in a multilayer film blowing machine.[4] Oriented drawn films were obtained by heating amorphous film to 80°C in a press, drawing to a draw ratio $\lambda$ of about 4, and rapidly cooling in air. Thermally crystallized films were obtained by annealing amorphous film in an air-circulating oven. IR spectra with a resolution of 2 $cm^{-1}$ were measured in transmission mode on a Nicolet Magna 860 Fourier transform instrument with a DTGS detector. To eliminate interference fringes, spectra were measured with the films tilted at the estimated Brewster angle of 57° and with polarization in the plane of incidence. For the drawn (oriented) samples, two spectra were measured, one with the machine direction in the plane of incidence and the other with the transverse direction in the plane of incidence. For uniaxial orientation, these two spectra can be used to calculate the true machine direction (MD) spectrum $S_M$ and the true transverse direction (TD) spectrum $S_T$, which is the same as the normal direction (ND) spectrum $S_N$ for uniaxial orientation. The structural factor spectrum $S_0$, which is independent of orientation effects, can then be calculated as $S_0 = (S_M + 2\ S_T)/3$. The equivalence of the TD and ND spectra (i.e. uniaxial orientation) was verified by repeating the analysis by means of the conventional tilted film technique, but these spectra contained some interference fringes. The following films were analyzed:

Am1 = Amorphous film about 5 μm thick
Am2 = Amorphous film about 25 μm thick
Dr1 = Film Am1 drawn at 80°C to $\lambda \sim 4$ (thickness ~ 3 μm)
Dr2 = Film Am2 drawn at 80°C to $\lambda \sim 4$ (thickness ~ 9 μm)
Cr1 = Film Am1 annealed at 120°C for 1 h
Cr2 = Film Am1 annealed at 160°C for 1 h
Cr3 = Film Am1 annealed at 200°C for 1 h

Factor analysis of spectra from these samples was performed with the use of the software GRAMS/386™ and PLSplus/IQ™ from Galactic Industries Corp.

In addition, two biaxially oriented industrial films Bi1 and Bi2 with thickness about 20 μm were examined; the conditions under which these films were prepared are not known.

## Results and Discussion

**Factor Analysis.** The spectra obtained from the samples prepared by us are shown in Figure 1; they have been normalized to a common intensity level based on the peak at 1410 $cm^{-1}$. For the drawn samples, only the structural factor spectra are shown. The spectrum of film Am2 was not included in the overall analysis because too many of the peaks were saturated, including those at 1410 and 1020 $cm^{-1}$; except for the intensity it was identical to that of film Am1. It should be noted that the transmittance spectra were converted into absorbance units without any correction for surface reflection. For precise analysis, the surface reflection should be taken into account and the spectra should be converted into units corresponding to the imaginary part of the molecular polarizability function, as was done by Cunningham et al.[5] The polarizability function was also used in our reflection work.[1] Unfortunately, this requires calculation of the index of refraction by means of the Kramers-Kronig transform, which was not possible in the present case because of missing data corresponding to the saturated peaks. However, the effect of neglecting this correction should be very small for the weaker peaks that are of most interest in this work.

In the 1800-600 $cm^{-1}$ region, where the spectra can be compared with those obtained by reflection on thicker samples,[1] the general behaviour is the same. On both drawing and thermal crystallization, peaks associated with *gauche* glycol conformers (1453, 1370, 1043, 899 $cm^{-1}$) diminish and are replaced by their *trans* counterparts (1471, 1340, 972, 849 $cm^{-1}$). However, as was the case for the samples analyzed in reflection, close inspection shows subtle differences in peak positions and shapes between the drawn samples and the thermally crystallized ones. Hence the set of six spectra shown in Figure 1 was submitted to factor analysis in a similar manner. Spectral regions corresponding to saturated peaks were excluded from the analysis. Again, as was the case for the reflection spectra, the analysis indicated the presence of three principal factors, which were then combined by means of spectral subtraction to generate three distinct spectra labelled G, TX, and TC. These are shown in Figure 2. They were normalized to a common intensity level based on the total area of the C–H stretching peaks at 3200 – 2700 $cm^{-1}$.

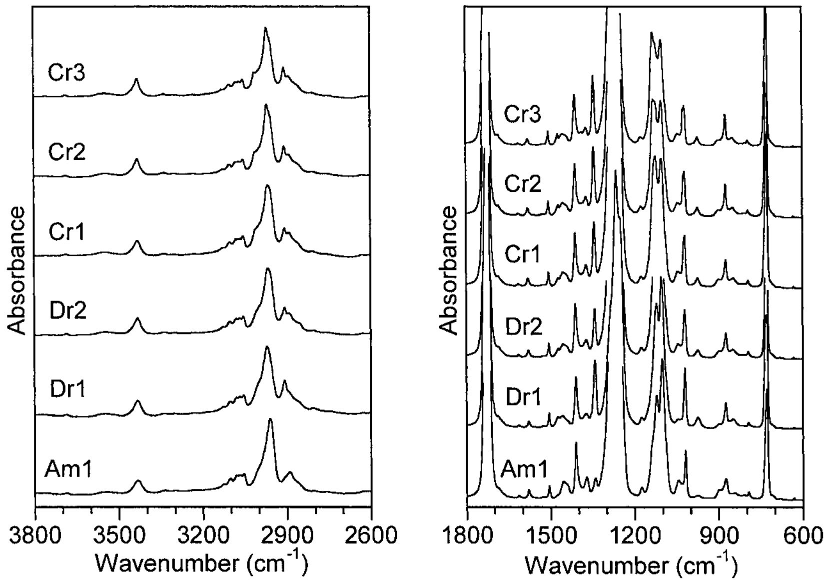

Figure 1. Transmission spectra of the set of films described in the Experimental section.

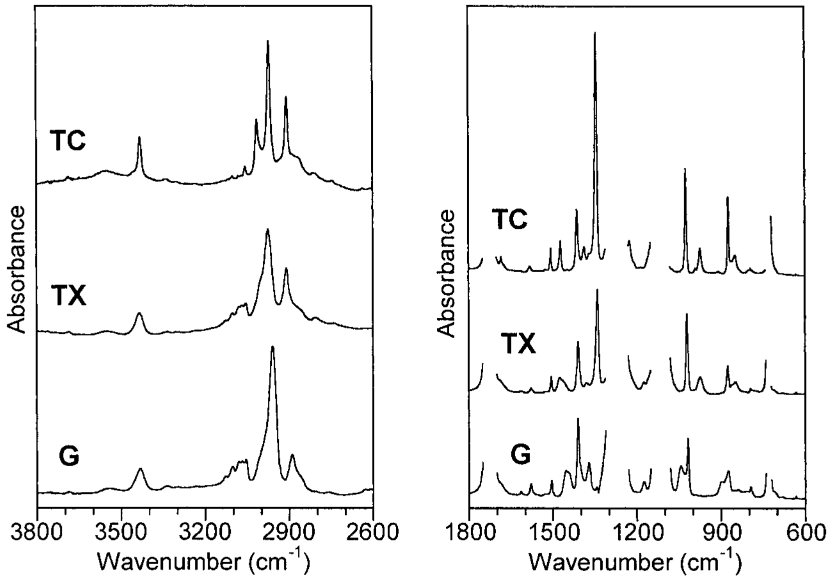

Figure 2. Basis spectra obtained by factor analysis.

From the scores produced by the factor analysis, combined with the coefficients relating our basis set to the primary factors, it was possible by means of matrix algebra to calculate the contributions of our three basis spectra to each of the experimental ones. The results, expressed on a percentage basis, are given in Table 1. As was observed for the thicker samples studied by reflection, drawing at 80°C produces mainly the disordered TX *trans* structure, while thermal crystallization produces more of the true crystalline TC *trans* structure.

Table 1. Breakdown of the experimental spectra in terms of the basis set.

| Sample | Description | % G | % TX | % TC |
|---|---|---|---|---|
| Am1 | Amorphous | 81.5 | 14.8 | 3.7 |
| Dr1 | Drawn at 80°C (3 μm thick) | 28.9 | 65.0 | 6.1 |
| Dr2 | Drawn at 80°C (9 μm thick) | 52.6 | 39.4 | 8.0 |
| Cr1 | Annealed at 120°C for 1 h | 50.9 | 32.5 | 16.6 |
| Cr2 | Annealed at 160°C for 1 h | 49.1 | 26.5 | 24.4 |
| Cr3 | Annealed at 200°C for 1 h | 49.7 | 21.7 | 28.6 |

In the 1800-600 $cm^{-1}$ region, the basis spectra are in excellent agreement with those obtained by reflection,[1] but they show finer details that will be discussed later. The high wavenumber region is especially interesting because it provides information that was not available from the reflection spectra. The G spectrum shows two strong glycol C–H stretching bands at 2959 and 2889 $cm^{-1}$, several aromatic C–H stretching bands between 3150 and 3040 $cm^{-1}$, and a carbonyl overtone band at 3432 $cm^{-1}$. In the TX spectrum, the change from glycol *gauche* to *trans* leads to a significant shift in the glycol C–H bands, to 2975 and 2909 $cm^{-1}$ respectively. However the aromatic C–H bands and carbonyl overtone remain unchanged, supporting our previous conclusion that the terephthalate group possesses the same disordered conformation in the TX structure as it does in the G structure. In the TC spectrum, on the other hand, the peaks occur at much the same positions as in the TX spectrum, but they are considerably more narrow, in keeping with the highly ordered structure of the true crystalline phase. Furthermore, an aromatic C–H stretching band at 3014 $cm^{-1}$ is now clearly resolved, but several other aromatic C–H bands have disappeared because of the centre of symmetry of the all-*trans* TC structure. Factor analysis of the C–H stretching region was done previously by

Koenig and coworkers. Koenig and Kormos published "gauche" and "trans" spectra that closely resemble our G and TC spectra.[6] Later, Liu and Koenig obtained three spectra that they assigned to "gauche", "amorphous trans", and "crystalline trans".[7] However, the difference between the two types of *trans* is not as clearly defined as in our TX and TC spectra, because their analysis involved only thermally crystallized samples with a relatively low content of the TX structure. The inclusion in the present work of drawn samples with a high content of the TX structure made it possible to achieve a cleaner separation of the three spectra.

Details of the low-wavenumber region are shown in Figure 3, which includes attempts at curve fitting. These figures may be compared with those published earlier for the reflection work, where the various peaks were discussed in detail.[1] In this paper only the differences will be discussed. In the 1540 – 1300 cm$^{-1}$ region, one important difference concerns the $CH_2$ deformation peak in the TX spectrum near 1470 cm$^{-1}$. In the earlier work this appeared to be a single broad band, but the transmission spectra show it to contain two components at 1476 and 1461 cm$^{-1}$. The G spectrum shows two components at 1455 and 1440 cm$^{-1}$, which Štokr et al. suggested might be due to Gt and Gg conformational arrangements.[3] The two components in the TX spectrum could similarly arise from Tt and Tg arrangements. However the TC spectrum, because it corresponds to an all-*trans* (Tt) arrangement, shows only a single (sharper) peak at 1471 cm$^{-1}$. Another difference concerns the $CH_2$ wagging peak near 1340 cm$^{-1}$. In both the TX and TC spectra this peak appears to contain a weak high-wavenumber component, but this may be an artefact arising from a slight asymmetry of this moderate-intensity peak caused by the lack of correction for surface reflection effects. In the 1080 – 940 cm$^{-1}$ region the transmission spectra very closely resemble the reflection ones, except that the in-plane benzene C–H peak in the TC spectrum at 1024 cm$^{-1}$ shows some low-wavenumber asymmetry. This could also arise from the lack of correction for surface reflection, or it could be due to incomplete elimination of the *gauche* contribution because of the presence of *gauche* conformers in the chain folds associated with the crystalline phase. In the 930 – 770 cm$^{-1}$ region, the transmission spectra are better defined than the reflection spectra, which showed a rather high noise level. However analysis is complicated because of the many overlapping peaks, and curve fitting must be approached with caution. The shift of the $CH_2$ rocking band at 900 cm$^{-1}$ in the G spectrum to 847 cm$^{-1}$ in the TX and TC spectra is clear, but the behaviour of the phenyl

C–H out-of-plane peak near 873 cm$^{-1}$ appears to be even more complex than indicated by the reflection spectra.

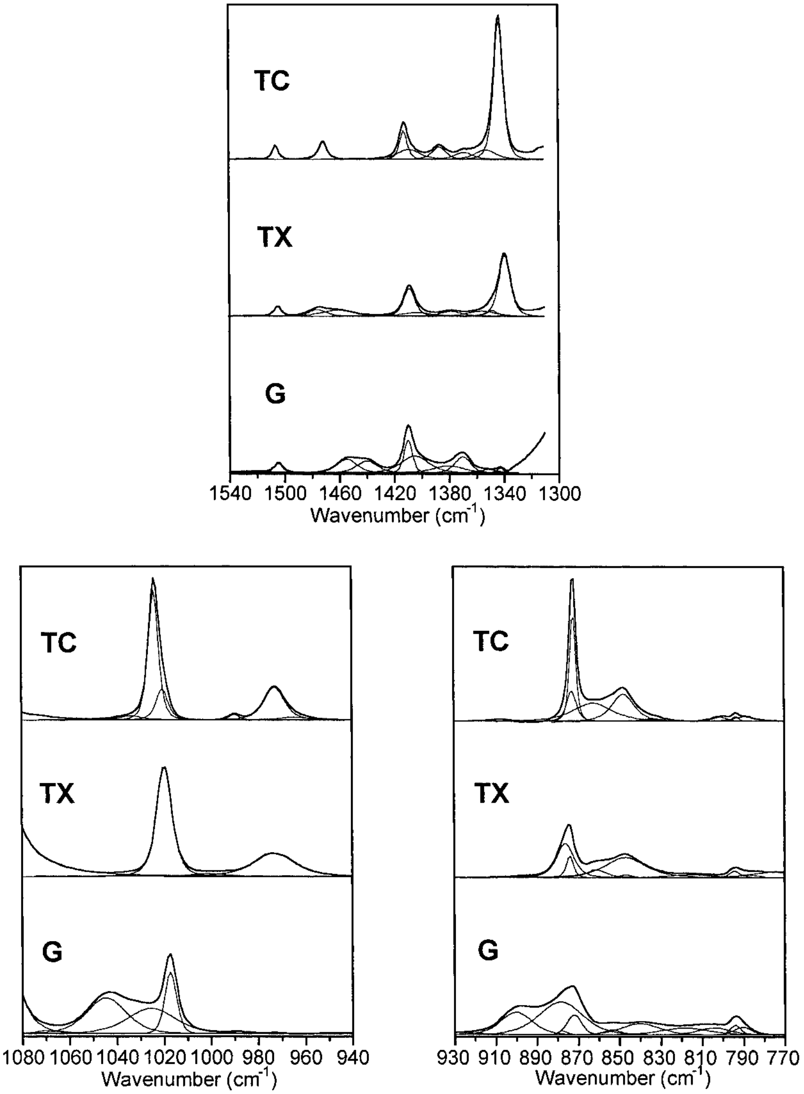

Figure 3. Details of basis spectra obtained by factor analysis.

In view of the new information provided by the transmission spectra, the band assignments published earlier have been updated and are given in Table 2.

Table 2. Peak parameters and assignments for PET based on results from this work and previous reflection work (Ref. 1). Peak positions are followed where possible by full peak width at half height (in parentheses), both in $cm^{-1}$.

| Band | G | TX | TC |
|---|---|---|---|
| C=O overtone | 3432 (33) | 3433 (30) | 3430 (11) |
| C–H stretch (aromatic) | 3127, 3103,<br>3080, 3068,<br>3054 | 3125, 3102,<br>3078, 3067,<br>3054 | 3055, 3014 |
| C–H stretch (glycol) | 2959, 2889 | 2975, 2909 | 2970, 2908 |
| C=O stretch | 1729 (22) | 1727 (22) | 1720 (16) |
| Ring def. | 1579 | 1577 | 1581 |
| Ring def. | 1504.6 (7.3) | 1504.9 (6.2) | 1506.1 (5.3) |
| $CH_2$ bending | 1455 (17) Gt?<br>1440 (17) Gg? | 1476 (15)<br>1461 (26) | 1472 (7) |
| Ring in-plane def. | 1410.0 (7.1) | 1408.8 (9.6) | 1412.5 (6.5) |
| ????? | 1405 (23) | 1403 (26) | 1409 (19) |
| Ring C–H in-plane def. | 1381 (26) | 1379 (17) | 1386 (12) |
| $CH_2$ wagging | 1370 (13) | 1340 (10) | 1343 (8) |
| Ring CCH | 1315 (21) | | |
| Ring-ester in-plane mode | 1287 (26) | | |
| Glycol O–C–H bending | 1266 (17) | 1270 (13) | 1278 (16) |
| Ring-ester in-plane mode | 1248 (20) | 1251 (20) | 1259 (19) |
| Ring mode or $CH_2$ twist | 1174 (18) | | |
| Ring mode or $CH_2$ twist | 1136 (23) | | |
| Ring-ester in-plane mode | 1120 (15) | 1124 (15) | 1132 (13) |
| In-plane ring mode | 1102 (16) | 1106 (13) | 1112 (9) |
| Glycol C–O stretching (sym) | 1092 (23) | 1091 (27) | |
| Glycol C–O stretching (antisym) | 1045 (20) Gt?<br>1026 (24) Gg? | 973 (20) | 973 (10) |
| Ring C–H in-plane def. | 1017.3 (5.8) | 1019.7 (7.6) | 1024.0 (4.9) |
| Chain folding | | | 990 (5) |
| $CH_2$ rocking | 900 (18) | 847 (23) | 848 (13) |
| Ring C–H out-of-plane def. | 873 | 874 | 872 |
| Ring C–H in-plane def. ? | 794 | 794 | 793 |
| Ring C–H + C=O out-of-plane def. | 730 (13) | 730 (9) | 726 (7) |

**Dichroism**. Further information on the spectrum and structure of PET was obtained from analysis of spectra measured with polarized radiation. Figure 4 shows the spectra of the uniaxially oriented sample Dr1 corresponding to polarization in the machine direction (MD) and the transverse direction (TD), as well as the difference spectrum obtained by subtracting the two. The latter is of great help in identifying the peaks that show significant dichroism. This thin film (about 3 μm thick) is of particular interest because it contains a large amount of the "disordered" *trans* structure TX and is also highly oriented, as can be seen from the strong dichroism exhibited in the difference spectrum of Figure 4. Nevertheless, the orientation is associated almost exclusively with the *trans* conformers, because peaks arising from the *gauche* conformers show very low dichroism. This is clear for the C–O stretch mode near 1040 cm$^{-1}$ and the $CH_2$ rocking mode at 900 cm$^{-1}$, but less so for the $CH_2$ deformation and wagging modes at 1450 and 1370 cm$^{-1}$ respectively. The reason can be seen on examination of the expanded graph of this region in Figure 4. The "bump" observed near 1370 cm$^{-1}$ in the difference spectrum is actually closer to 1380 cm$^{-1}$ and arises from the dichroism of the ring mode of the TX structure, which is usually hidden under the 1370 cm$^{-1}$ peak. For the deformation modes, the *gauche* peaks at 1455 and 1440 cm$^{-1}$ show negligible dichroism, but the TX peaks at 1476 and 1461 cm$^{-1}$ show perpendicular dichroism in the first case (negative peak in the difference spectrum) and parallel dichroism in the second (positive peak). This makes dichroic analysis of this region rather complicated. A similar situation arises for the in-plane ring mode near 1410 cm$^{-1}$. For the TX structure this peak occurs at 1409 cm$^{-1}$ and shows slight parallel dichroism. For the TC structure it occurs at 1412 cm$^{-1}$ and shows perpendicular dichroism. In Figure 4 the net result, given the rather low amount of TC structure, is a maximum at 1407 cm$^{-1}$. In the C–H stretching region, the difference spectrum shows definite parallel dichroism for peaks at 2975 and 2909 cm$^{-1}$; both correspond exactly to the TX structure and not the G structure.

Of the remaining peaks, the two out-of-plane ring modes at 873 and 727 cm$^{-1}$ show perpendicular dichroism, as expected, and the others show parallel dichroism. For the peaks at 1340, 1020, and 973 cm$^{-1}$, which are relatively isolated from other peaks, it is possible to calculate reasonably accurate dichroic ratios $D$ and subsequently orientation functions $f$, if the angle $\alpha$ between the vibration's transition moment and the molecular chain is known. The values obtained are given in Table 3. For the *trans* peak at 1340

$cm^{-1}$, taking the reported value[8] of 21° for $\alpha$ leads to $f$ = 1.05, which is higher than the physically allowable maximum value of 1. However, a slight adjustment to 18°, within experimental error, brings the value down to 1. If $\alpha$ is assumed to be 0°, a value of 0.85 is obtained for $f$; this corresponds to the minimum possible value. For the *trans* peak at 973 $cm^{-1}$, taking the reported value[8] of 34° for $\alpha$ leads to $f$ = 1.30. This is physically impossible and this value for $\alpha$ appears to be an overestimation. To bring $f$ down to below 1 requires that $\alpha$ be 27° or less. The value of 19° suggested by other workers[9,10] gives $f$ = 0.82. The peak near 1020 $cm^{-1}$ contains a component at 1017 $cm^{-1}$ arising from the G structure and one at 1020 $cm^{-1}$ arising from the TX structure. The dichroism arises mainly from the 1020 $cm^{-1}$ component and the dichroic ratio for this component was determined both by interactive spectral subtraction and by curve fitting. The reported value[11] of 20° for $\alpha$ gives $f$ = 0.96 whereas a value of 0° gives $f$ = 0.79. Thus the orientation function for the *trans* groups in film Dr1 must lie between 0.8 and 1. A value near 1 is more likely, since it is in better agreement with reported $\alpha$ values, except for the peak at 973 $cm^{-1}$.

Table 3. Dichroic ratios and calculated orientation functions for the drawn film Dr1.

| Peak and Dichroic Ratio D | Transition Moment Angle $\alpha$ | Orientation Function $f$* |
|---|---|---|
| 1340 $cm^{-1}$ ($CH_2$ wag)<br>D = 18.1 | 21° (Ref. 8)<br>18°<br>0° | 1.05<br>0.99<br>0.85 |
| 973 $cm^{-1}$ (C–O stretch)<br>D = 7.74 | 34° (Ref. 8)<br>27°<br>19° (Refs. 9, 10) | 1.30<br>1.00<br>0.82 |
| 1020 $cm^{-1}$ (C–H in-plane, TX component)<br>D = 12.4 | 20° (Ref. 11)<br>0° | 0.96<br>0.79 |

$$*\, f = \frac{D-1}{D+2}\cdot\frac{2}{3\cos^2\alpha - 1}$$

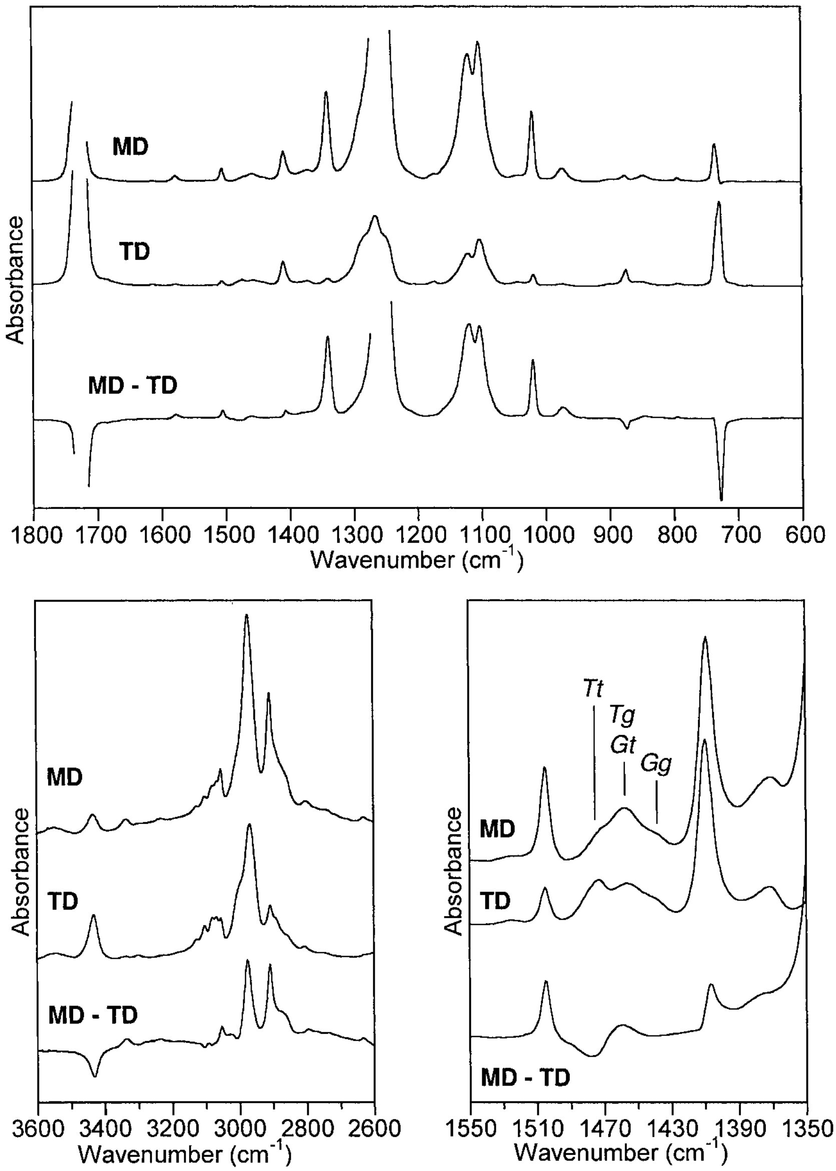

Figure 4. Dichroic spectra and difference spectrum for drawn film Dr1.

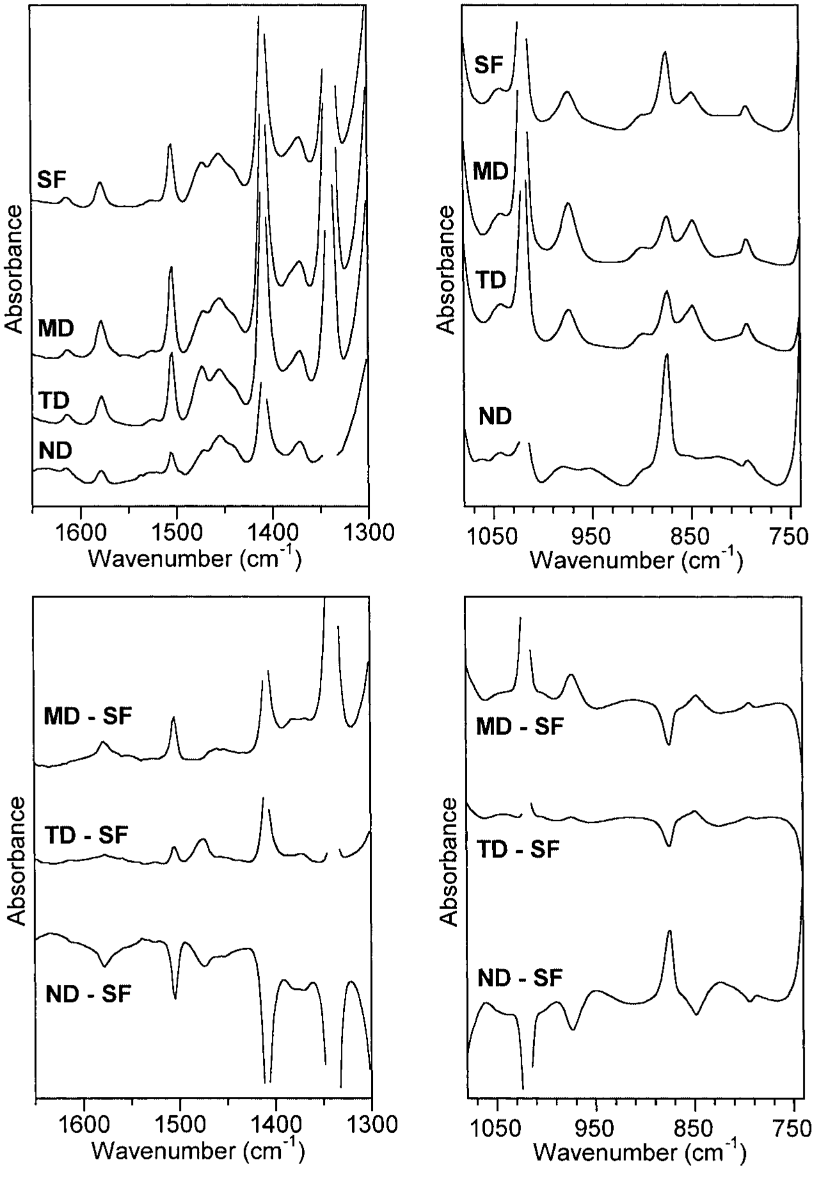

Figure 5. Trichroic spectra (top) and difference spectra (bottom) for the biaxially oriented film Bi1.

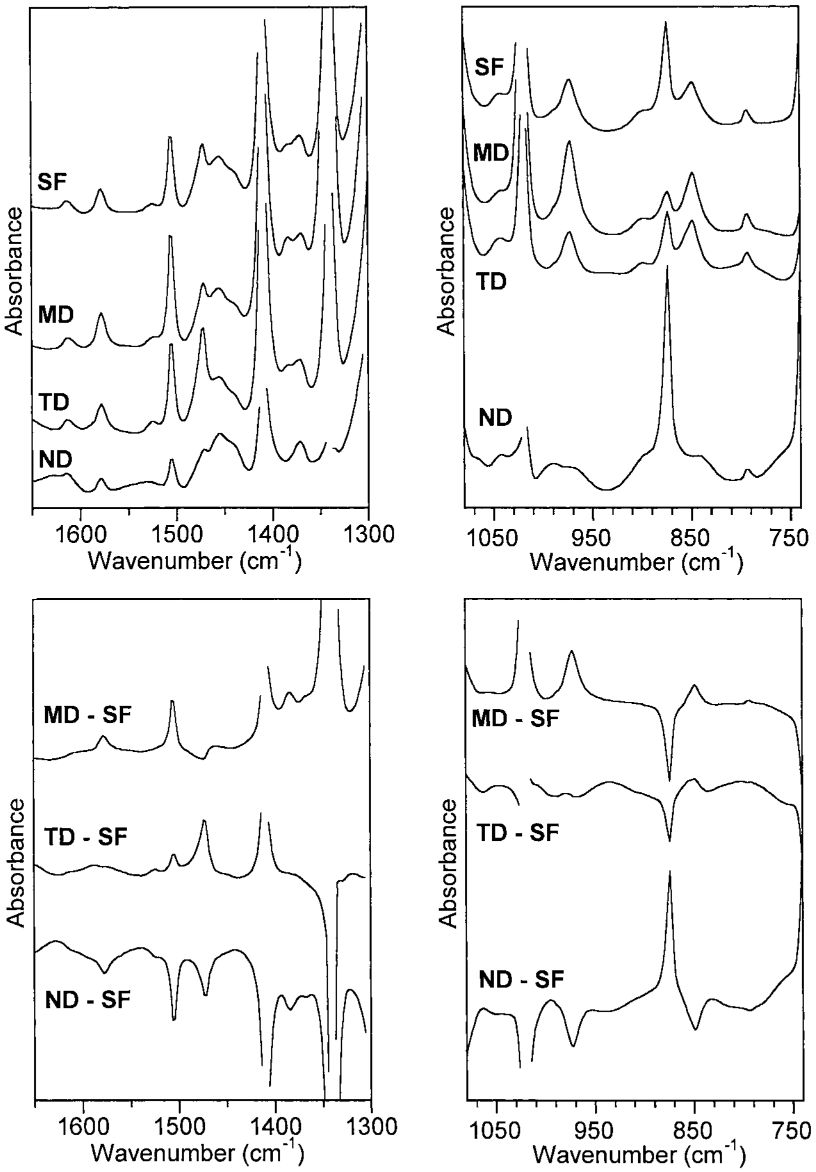

Figure 6. Trichroic spectra (top) and difference spectra (bottom) for the biaxially oriented film Bi2.

Figure 5 shows the spectra obtained for the oriented industrial film Bi1. In this case the analysis was done by the conventional tilted film method and confirmed that the orientation was biaxial, so the Brewster angle approach could not be used. The figure shows the trichroic spectra corresponding to the three orthogonal directions MD, TD, and ND, as well as the structural factor spectrum SF and the difference spectra MD – SF, TD – SF, and ND – SF. Because of the film thickness (about 20 μm) even the peaks at 1410, 1340, and 1020 cm$^{-1}$ are saturated, but nevertheless information about the trichroic behaviour of these peaks can be obtained.

This film exhibits some very interesting characteristics. First of all, as for the uniaxially drawn film, the peaks specifically associated with the *gauche* glycol conformers (1455, 1440, 1370, 1043, 899 cm$^{-1}$) show that they are not highly oriented; these peaks are weak in the difference spectra. Second, the out-of-plane ring C–H modes at 873 and 727 cm$^{-1}$, which have their transition moments normal to the ring plane, are much stronger in the ND spectrum than in the MD and TD spectra. This indicates that the benzene rings are preferentially oriented in the plane of the film, a phenomenon that has been reported previously.[12] Third, the remaining peaks are much weaker in the ND spectrum than in the other two. This is especially true for peaks specifically associated with the *trans* glycol conformers (1340, 973, 847 cm$^{-1}$), which are practically absent from the ND spectrum. For a planar molecular structure, the $CH_2$ wagging mode at 1340 cm$^{-1}$ and the C–O stretching mode at 973 cm$^{-1}$ are expected to have their transition moments in the plane. Thus their behaviour indicates that the *trans* structures present in this film are in planar units that have their planes highly oriented in the plane of the film. The in-plane aromatic ring vibrations at 1577, 1505, 1410, 1020, and 793 cm$^{-1}$ show behaviour similar to that of the *trans* peaks, but the effect is not as pronounced because they also include contributions from the weakly oriented *gauche* structures. Of the in-plane vibrations, most of the peaks (1577, 1505, 1380, 1340, 1020, 973, 793 cm$^{-1}$) are significantly stronger in the MD spectrum than in the TD spectrum. These are vibrations with transition moments parallel or close to the molecular chain, and they show that the molecular chains are more oriented towards the machine direction than the transverse direction. However, the $CH_2$ deformation mode at 1470 cm$^{-1}$ shows the opposite behaviour (stronger in the TD spectrum than in the MD spectrum, and weakest in the ND spectrum) because its transition moment lies in the molecular plane but perpendicular to the chain. The peaks at 1410 and 847 cm$^{-1}$ have similar intensity in the

MD and TD spectra; these are vibrational modes whose transition moment must be close to 55° with respect to the chain ($3 \cos^2\alpha - 1 \sim 0$). This is why the 1410 $cm^{-1}$ peak is often assumed to be insensitive to orientation. However, because this is an in-plane vibration, this assumption is incorrect in cases like the present one where there is preferential orientation of the molecular planes. A final important point concerning this film is that comparison of its spectra with the basis spectra obtained by factor analysis indicates that it contains a high content of the TX structure. By subtraction of the basis spectra from the structural factor (SF) spectrum, the composition was estimated to be 38% G, 59% TX, 3% TC. The orientation effects observed strongly suggest that the molecular chains are planar. This in turn implies that the TX structure involves *cis* and *trans* arrangements of the terephthalate group rather than out-of-plane arrangements.

It is interesting to compare the spectra obtained for the second biaxial film Bi2, shown in Figure 6. Although the general behaviour is similar in terms of orientation, there is one important difference: this film has a higher content of the true crystalline TC structure. This is clear from the sharper peaks at 1471 and 873 $cm^{-1}$, and from the distinct peak at 1386 $cm^{-1}$. By spectral subtraction the composition was estimated to be 26% G, 59% TX, and 15% TC. Thus while at first glance films Bi1 and Bi2 may appear to be very similar, when they are examined more closely in the light of the results of this work, they are found to be structurally quite different.

For both of these films, the behaviour of the $CH_2$ rocking peak near 848 $cm^{-1}$ peak is difficult to explain. As pointed out by Krimm,[13] the $CH_2$ deformation, wagging, and rocking modes should be mutually perpendicular to a first approximation. Since the wagging mode at 1340 $cm^{-1}$ appears to be in-plane and parallel to the chain (as expected), and the deformation mode at 1470 $cm^{-1}$ appears to be in-plane and perpendicular to the chain (again as expected), the rocking mode should be out-of-plane. However it appears to be almost perfectly in-plane. This band may have been wrongly assigned, but there is no other obvious out-of-plane mode that could be assigned in its place. The C–H stretching modes also show anomalous behaviour, since they show parallel dichroism rather than the perpendicular dichroism expected from the crystal structure.[9,13] This is confirmed by the spectra of Figure 4. There are thus several questions to be answered concerning the IR spectrum of PET, and consideration of the possible structures may be of help in this respect. For instance, Figure 7 compares a hypothetical all-*cis* planar structure with the true crystalline all-*trans* structure. The all-

*cis* structure can give rise to reasonably linear chains with a well-defined chain axis. However, the transition moment angles of the different vibrations with respect to the chain axis can be quite different for the two structures. For example, a vibration with its transition moment along the *para* axis of the benzene ring will have α ~ 16° for the all-*trans* structure but α = 0° for the all-*cis* structure. The TX structure proposed by us for the "intermediate" phase of PET may involve a mixture of *cis* and *trans* terephthalate conformations, and will be intermediate between the two structures shown in Figure 7 in terms of transition moment angles.

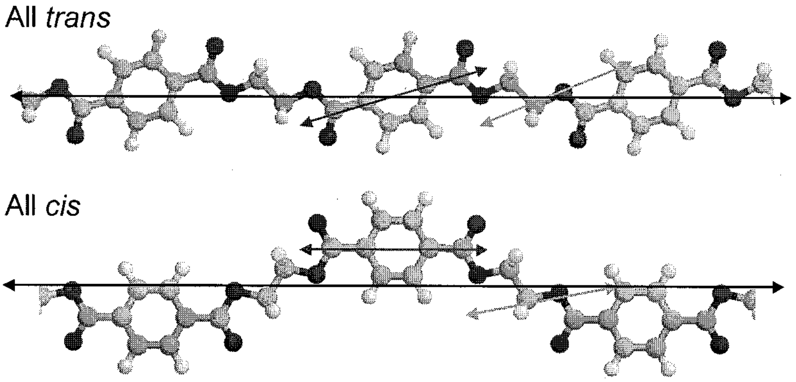

Figure 7. Illustration of all-*trans* arrangement found in crystalline PET and hypothetical all-*cis* arrangement.

## Conclusions

The results obtained by transmission spectroscopy of thin films in this work confirm the conclusions reached in our earlier reflection work, namely that PET contains three major distinct structures. The first, designated G, is found mainly in the amorphous phase and contains *gauche* glycol conformers in combination with disordered terephthalate segments. The second, designated TX, contains *trans* glycol conformers in combination with disordered terephthalate segments. It corresponds to isolated *trans* units found in the amorphous phase as well as extended *trans* sequences found especially in drawn samples but also in thermally crystallized ones. The third, designated TC, corresponds to the true crystalline phase of PET and contains *trans* glycol conformers as well as ordered *trans* terephthalate segments. The spectra corresponding to these three structures have been defined in greater detail as a result of the transmission work. The strong orientation of molecular planes observed in an industrial film containing a high content of the TX structure suggests that the TX structure is close to planar, i.e. the disordered terephthalate groups probably involve a mixture of *cis* and *trans* units rather than out-of-plane arrangements. The results obtained in this work open up new possibilities for characterizing the structure and orientation of PET in greater detail by IR spectroscopy, but the different structures present and the possibility of different transition moment angles for these structures mean that analysis of the orientation will be rather complicated and will require some effort.

## References

[1] K. C. Cole, A. Ajji, E. Pellerin, submitted to *Macromolecules*.
[2] R. de P. Daubeny, C. W. Bunn, C. J. Brown, *Proc. Roy. Soc. (London)* **1954**, *226A*, 531.
[3] J. Štokr, B. Schneider, D. Doskocilová, J. Lövy, P. Sedlácek, *Polymer* **1982**, *23*, 714.
[4] X. Zhang, A. Ajji, J.-M. Verilhac, *Polymer* **2001**, *42*, 8179.
[5] A. Cunningham, I. M. Ward, H. A. Willis, V. Zichy, *Polymer* **1974**, *15*, 749.
[6] J. L. Koenig, D. Kormos, *Contemporary Topics in Polymer Science* **1979**, *3*, 127.
[7] J. Liu, J. L. Koenig, *Anal. Chem.* **1987**, *59*, 2609.
[8] P. Spiby, M. A. O'Neill, R. A. Duckett, I. M. Ward, *Polymer* **1992**, *33*, 4479.
[9] C. Y. Liang, S. Krimm, *J. Mol. Spectrosc.*, **1959**, *3*, 554.
[10] G. K. Kuznetsov, L. V. Belekhin, M. G. Kamenskii, *Mech. Compos. Mater.* **1985**, *21*, 378.
[11] I. J. Hutchinson, I. M. Ward, H. A. Willis, V. Zichy, *Polymer* **1980**, *21*, 55.
[12] P. Lapersonne, D. I. Bower, I. M. Ward, *Polymer* **1992**, *33*, 1266.
[13] S. Krimm, *Adv. Polym. Sci.* **1960**, *2*, 51.